Proc. Natl. Acad. Sci. USA
Vol. 78, No. 3, pp. 1656–1660, March 1981
Biophysics

Acoustic microscopy of living cells

(ultrasound/elastic properties/cell motility)

J. A. HILDEBRAND*, D. RUGAR*, R. N. JOHNSTON†, AND C. F. QUATE*‡

*Edward L. Ginzton Laboratory and †Department of Biological Sciences, Stanford University, Stanford, California 94305

Contributed by C. F. Quate, December 10, 1980

ABSTRACT **This paper reports preliminary results of the observation by acoustic microscopy of living cells *in vitro*. The scanning acoustic microscope uses high-frequency sound waves to produce images with submicrometer resolution. The contrast observed in acoustic micrographs of living cells depends on the acoustic properties (i.e., density, stiffness, and attenuation) and on the topographic contour of the cell. Variation in distance separating the acoustic lens and the viewed cell also has a profound effect on the image. When the substratum is located at the focal plane, thick regions of the cell show a darkening that can be related to cellular acoustic attenuation (a function of cytoplasmic viscosity). When the top of the cell is placed near the focal plane, concentric bright and dark rings appear in the image. The location of the rings can be related to cell topography, and the ring contrast can be correlated to the stiffness and density of the cell. In addition, the character of the images of single cells varies dramatically when the substratum upon which they are grown is changed to a different material. By careful selection of the substratum, the information content of the acoustic images can be increased. Our analysis of acoustic images of actively motile cells indicates that leading lamella are less dense or stiff than the quiescent trailing processes of the cells.**

The scanning acoustic reflection microscope is a novel way of investigating biological materials with submicrometer resolution. The information content of acoustic images differs from that of optical or electron microscopic images. Acoustical images contain information about mechanical properties of the object: density, stiffness, and acoustic attenuation. An acoustic microscope with water as the coupling medium has been used to image subcellular detail in fixed cells (1). A liquid argon-coupled acoustic microscope has been used to image human metaphase chromosomes with a resolution of 0.38 μm (2). In this paper we present preliminary results of the observation of living cells *in vitro*. We have found that living cells can be viewed for several hours with no apparent disruption. The cells continue to exhibit normal patterns of motility and remain well spread on the substratum. It appears that neither the high-frequency sound waves nor the mechanical scanning cause significant cellular damage. Living cells are particularly interesting for study because little is known about the mechanical properties of a single cell and their relations to cell behavior.

The acoustic microscope used in this study was developed by Lemons and Quate (3) and was modified to operate as a reflection instrument at nearly opitcal wavelengths by Jipson and Quate (4). The basic operation of a reflection acoustic microscope can be understood with reference to Fig. 1. A radio-frequency electrical pulse is used to excite a thin-film piezoelectric transducer located at one end of a sapphire crystal. The transducer generates an acoustic plane wave which propagates through the sapphire crystal to a spherical lens with a large opening angle. The spherical interface focuses the acoustic beam to a diffraction-limited spot in the liquid (5). A portion of the acoustic energy is reflected by the object. The reflected acoustic waves are collected by the lens and converted back into an electrical signal by the transducer. The detected acoustic power determines the brightness of a picture element in the acoustic micrograph. The acoustic image of the object is formed point-by-point as the object is mechanically scanned in a raster pattern. The time to record an image is typically 30 sec. The image is visually displayed on a cathode-ray-tube screen and the face of that screen is photographed to preserve the image.

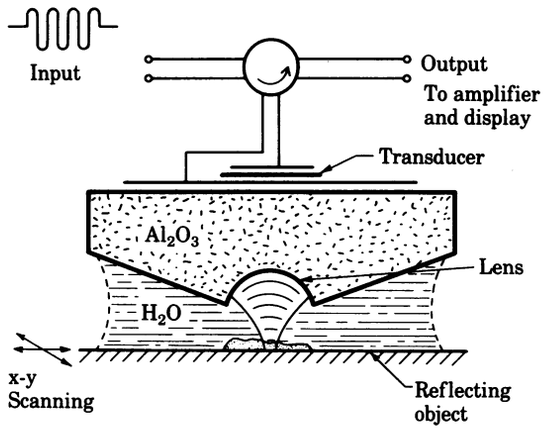

FIG. 1. Illustration of the operation of the scanning reflection acoustic microscope.

The contrast observed in reflection acoustic images is a function of the mechanical properties of the object and of lens-to-object spacing. When living cells are imaged, the acoustic return is typically maximal when the surface of the substratum is located in the focal plane of the lens. We define this position as $Z = 0$. The mathematical notation for the acoustic lens output voltage as a function of focal position has been called $V(Z)$ by Atalar (6) and acoustic material signature by others (7). The measured $|V(Z)|^2$ curve for a quartz substratum is shown in Fig. 2.

MATERIALS AND METHODS

Cell Culture. Heart ventricles of embryonic chickens (8–10 days of incubation) were dissociated into suspensions of single cells with 0.25% trypsin (Microbiological Associates, Bethesda MD). The cells were then incubated in humidified 5% CO_2/95% air at 37°C in Eagle's minimal essential medium (GIBCO F-12) supplemented with 10% (vol/vol) fetal bovine serum

The publication costs of this article were defrayed in part by page charge payment. This article must therefore be hereby marked "*advertisement*" in accordance with 18 U. S. C. §1734 solely to indicate this fact.

Abbreviation: dB, decibels.

‡ To whom reprint requests should be addressed.

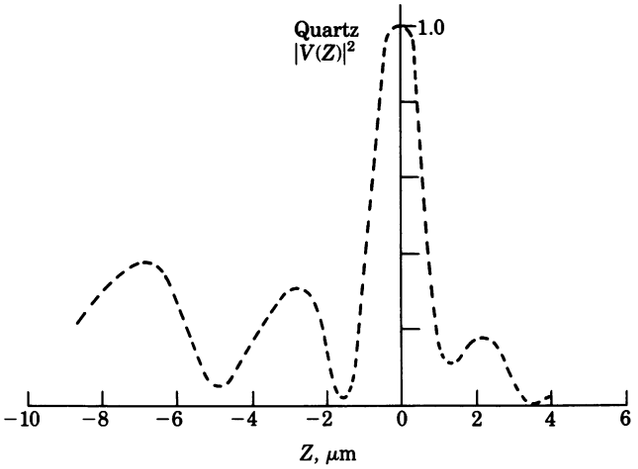

FIG. 2. The measured power output $|V(Z)|^2$ of the acoustic microscope as a function of the focal position of a quartz (fused silica) substratum. The acoustic lens used to obtain this curve also was used to record the images in this paper.

(Microbiological Associates) for 2–5 days. The cells were grown on various sterile substrata, including fused silica (quartz), glass-on-sapphire, and polystyrene 35-mm-diameter Falcon tissue culture dishes.

Living Cell Microscopy. The culture dish was transferred to the acoustic microscope for imaging. To minimize acidity changes, the cells were bathed in culture medium buffered with 10 mM Hepes (GIBCO) just before being placed in the microscope. This medium served to couple the sound from the acoustic lens to the cells. No significant difference was observed between the acoustic properties of the medium and those of distilled water. The acoustic lens was maintained at 37°C, but otherwise the medium was not heated after it was placed in the microscope. The limiting frequency of the acoustic microscope is determined by the attenuation over the liquid path length. At 37°C we are able to operate at 1.7 GHz with a 31-μm-radius lens (f/0.75) and to observe a signal-to-noise ratio in excess of 40 decibels (dB). This results in an acoustic wavelength of 0.9 μm and a Rayleigh criterion resolution of 0.72 μm.

LIVING CELLS ON VARIOUS SUBSTRATA

The character of acoustic images of cells is dependent on the nature of the underlying substratum. The important parameters of the substratum are the acoustic impedance and the shape of the $V(Z)$ curve. Acoustic impedance is a term used to denote the product of density and velocity or, similarly, the square root of the stiffness-density product. It plays an important role in the equations that determine the amount of acoustic power transferred across the interface between two materials. Images of living cells on three different substrata are considered.

Quartz. Images of a cell on a quartz substratum at three different focal positions are shown in Fig. 3. Quartz has a higher acoustic impedance than either the cell or the liquid medium. At a water/quartz interface, a plane wave at normal incidence will experience a 65% power reflection, whereas the power reflected at a water/cell interface is probably less than 0.5%. In Fig. 3*a*, the liquid/quartz interface is located in focus. There the quartz reflection dominates the observed acoustic return. The main effect of the cell is to attenuate the sound on its way to and from the quartz. The background is bright, while the interior of the cell shows a steady darkening as the cell becomes thicker. This indicates that the acoustic attenuation of the cell is somewhat greater than that of the liquid medium.

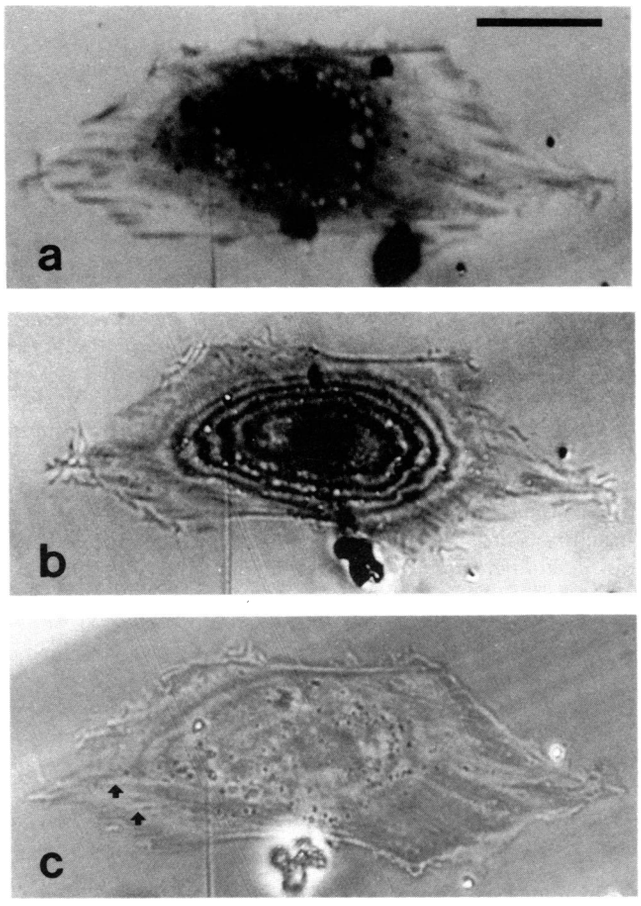

FIG. 3. Acoustic images of a chicken heart fibroblast on a quartz substratum at three different focal positions. (*a*) When the substratum is placed in focus, it appears bright while the thick interior of the cell appears dark. Two nuclei are visible in the dark region, while both bright and dark particles are observed in a ring around the nuclei. Dark streaks are observed along the cell margin which may represent sites of cell-to-substratum attachment. (*b*) At increased lens-to-substratum separation ($Z = 1.3$ μm), the cell image exhibits rings of contrast. The rings are an interference between the acoustic reflection from the top of the cell and that from the substratum, and they are correlated with cell topography. (*c*) For lens-to-substratum spacings decreased from focus ($Z = -1.6$ μm), the cell image is a uniform grey with slightly increased contrast for the cell margin. The arrows show intracellular fibers which appear as bright streaks. Bar = 20 μm.

Fig. 3*b* shows the same cell imaged with the lens-to-substratum spacing increased beyond focus ($Z = 1.3$ μm). The image exhibits rings of contrast, which are faint where the cell is thin and become more distinct as the cell becomes thicker. The rings are a consequence of interference between the reflection from the top of the cell and the reflection from the substratum. Because the reflection from the substratum must pass twice through the cell, its phase is determined by the ratio of cell thickness to acoustic velocity. Along a dark ring the two reflections are exactly out of phase, resulting in maximum cancellation. For positive Z focal positions, the reflection from the substratum is reduced because it is out of focus. For increasingly thick cellular regions, the top of the cell is located closer to the focal plane and, thus, reflects more power. The two reflections then become comparable in size and interfere to produce increasingly bright and dark rings. Ring contrast may be a useful indicator of cellular mechanical properties. The size of the reflection from the top of the cell varies as a function of cytoplasmic impedance. High impedance leads to a large reflection from the top of the cell and to more contrast in the rings.

Fig. 3*c* presents an image with lens-to-quartz spacing decreased from the focus ($Z = -1.6$ μm). The reflection from the quartz has been minimized by adjusting the focal setting to a minimum of the $V(Z)$ (Fig. 2). The image has increased contrast for the cell margin. Bright linear features, which may be intracellular fibers, appear in some regions where they are only faintly detected in the $Z = 0$ image (Fig. 3*c*, arrows).

Polystyrene. Polystyrene has an impedance that is close to that of water. At a water/polystyrene interface, the power reflection coefficient is 6% for normally incident plane waves. The measured $|V(Z)|^2$ for the bottom of a polystyrene culture dish is shown in Fig. 4. The peak of the $|V(Z)|^2$ for polystyrene is reduced by a factor of 14 from the peak of the quartz $|V(Z)|^2$. On a polystyrene substratum, the reflection from the cell becomes a larger fraction of the total received acoustic signal.

The images of Fig. 5 show cells on a polystyrene substratum at two different focal positions. The reduced substratum reflection produces an enhanced ring contrast in the positive focal position image (Fig. 5*a*). At $Z = 0$, a complicated intracellular structure is observed whose linear features may represent cytoskeletal fibers and sites of attachment of the cell to the substratum. The nature of these images is reminiscent of those seen by interference-reflection microscopy (e.g., see ref. 8).

Quarterwave Glass-on-Sapphire. Finally, we designed a substratum with an antireflection coating of glass one-quarter wavelength in thickness deposited on top of a sapphire crystal. The glass layer serves to couple sound from the water into the sapphire. Fig. 6 shows the experimentally measured $|V(Z)|^2$ for a quarterwave glass-on-sapphire substratum. Notice that the peaks of the $|V(Z)|^2$ curve increase away from the focus unlike quartz or polystyrene. The $Z = 0$ peak of reflected power for a quarterwave glass-on-sapphire substratum is a factor of 2.4 less than for a quartz substratum. At $Z = -1.1$ μm from focus, the glass-on-sapphire has a deep minimum in reflected power that is a factor of 55 smaller than at focus.

Images of cells on a quarterwave glass-on-sapphire substratum at the $Z = -1.1$ μm focal position are shown in Fig. 7. These cells were imaged for 2 hr without apparent damage and exhibited normal patterns of motility. Both advance of the cell margin in the form of leading lamellae and retraction of extended processes were observed (9). The nucleolus of each cell is visible as a darkened region inside the nucleus. The dark margin seen at the bottom extension of the cell in Fig. 7*d* is believed to be the result of ruffling (10). The ruffle acts to scatter the acoustic beam creating a dark region in the image. Small particles, which may be lysosomes or lipid granules (11), are also seen within the cells. Both bright and dark particles are observed at the $Z = -1.1$ μm focal position. The observed dif-

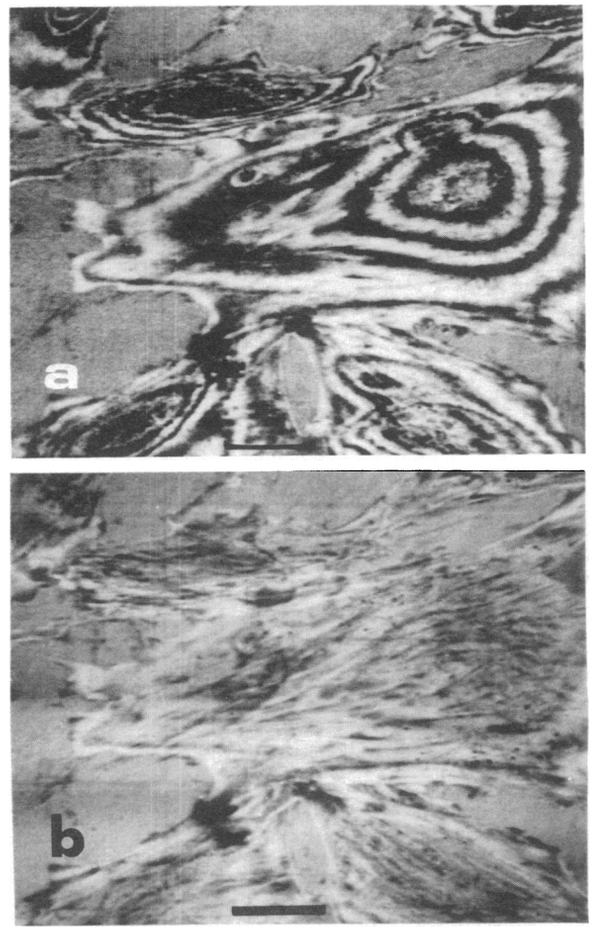

FIG. 5. Acoustic images of a cluster of cells on a polystyrene substratum. (*a*) Because of the reduced impedance of polystyrene, an enhanced ring structure is observed for increased lens-to-substratum spacing ($Z = 1.3$ μm). (*b*) At a different focus, $Z = 0$, a structure is observed that may correspond to intracellular fibers and sites of cell–substratum adhesion. Bar = 20 μm.

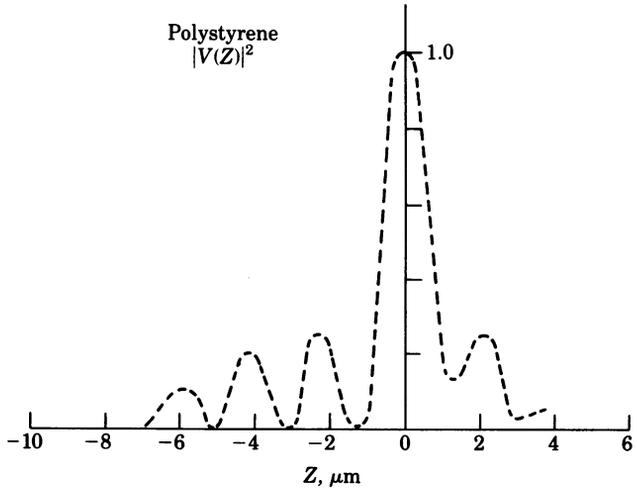

FIG. 4. The measured power output $|V(Z)|^2$ of the acoustic microscope as a function of focal position for a polystyrene substratum.

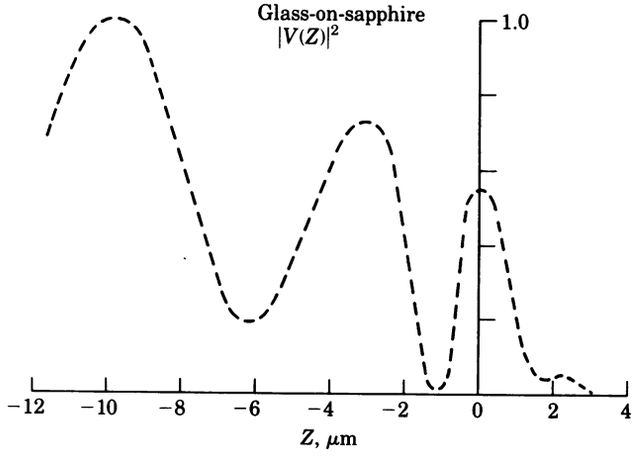

FIG. 6. The measured power output $|V(Z)|^2$ of the acoustic microscope as a function of focal position for a quarterwave glass-on-sapphire substratum.

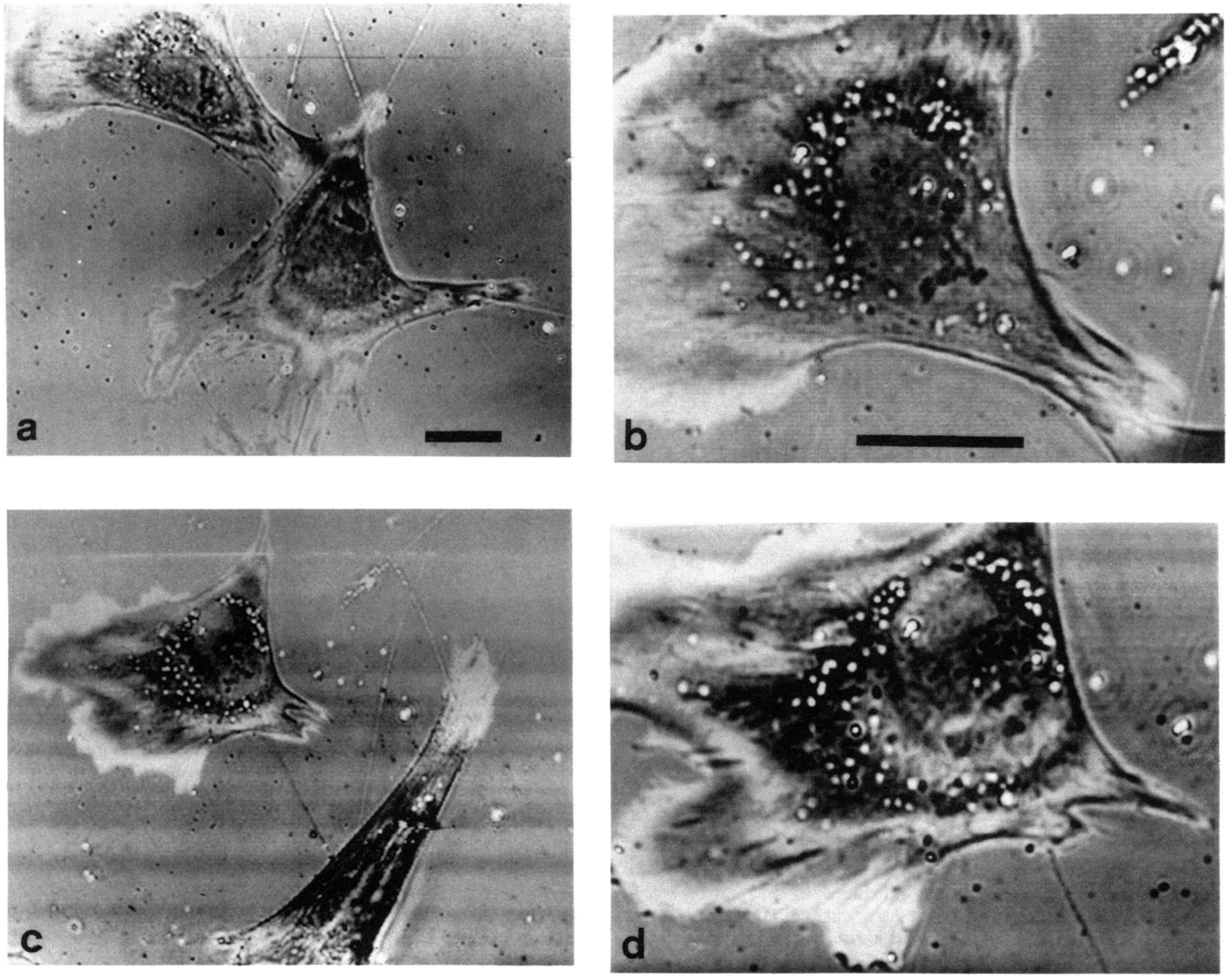

FIG. 7. Acoustic micrographs of cells on a quarterwave glass-on-sapphire substratum at a focal position that gives minimum substratum reflection ($Z = -1.1$ μm); selected images of a pair of cells that were viewed continuously for about 2 hr. Throughout this period, the cells exhibited apparently normal patterns of motility. Many intracellular organelles, such as nuclei, mitochondria, and lipid or lysosomal bodies are visible. The small spots seen on the bare substratum are holes in the deposited glass layer. These can serve as markers to gauge cellular motion. Times follow: 0 min (*a*); 25 min (*b*); 68 min (*c*); 83 min (*d*). *b* and *d* are images of the upper cell of *a* and *c* at twice the magnification. Bars = 20 μm.

ferences in returned acoustic signal for these particles may be a function of their focal positions.

Fig. 8 shows an image of the upper cell of Fig. 7 taken at $Z = -0.5$ μm focal position. Comparison of Figs. 7*b* and 8 (6-min separation) illustrates the dramatic effect of focal position on the character of the observed image. The dark streaks seen in Fig. 8 are consistent with the shape and distribution of focal contacts (12). They are located near the edge of the extended process at the top of the cell and under the peripheral regions of the leading lamella on the left. They are less than 1 μm in width and range up to 10 μm in length. It has been reported that regions of focal contact have 10- to 15-nm separation between the cell and substratum, whereas other regions of the cell have greater cell-to-substratum separation (12). By using a plane-wave model for the acoustic microscope beam which considers only the three largest reflections (the top of the cell, the bottom of the cell, and the substratum), it can be shown that for cell-to-substratum spacings from 0 to 224 nm, the total reflection increases with increased spacing. Thus, acoustic images should darken at focal contacts, and this appears to be confirmed in Fig. 8. A preliminary comparison of sequential acoustic images and interference-reflection contrast images of single cells supports

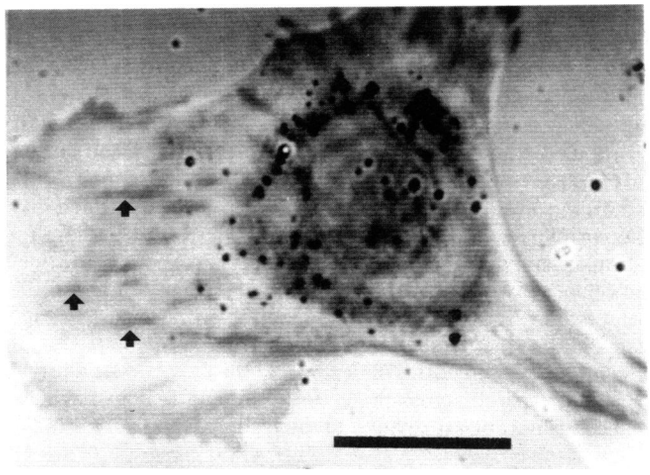

FIG. 8. Possible sites of cell-to-substratum attachment appear as dark streaks (arrows) in this image at the $Z = -0.5$ μm focal position of a quarterwave glass-on-sapphire substratum. Comparison with Fig. 7*b*, which is an image of the same cell 6 min earlier, shows the dramatic dependence of image contrast on focal position. Bar = 20 μm.

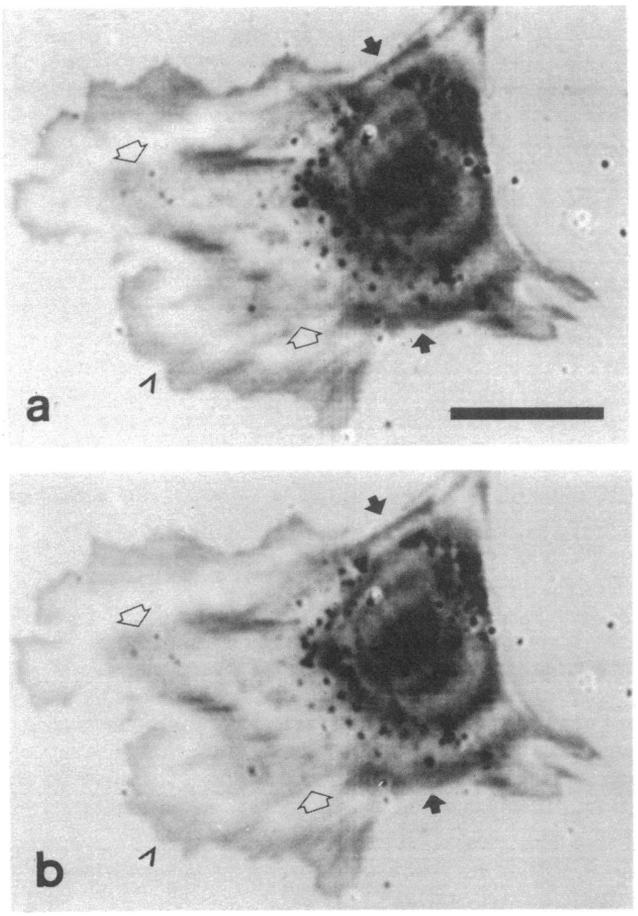

FIG. 9. Ring contrast and cell motility. These images are of the same cell shown in Figs. 7 and 8 and were prepared at 70 min (*a*) and 73 min (*b*). Active motility is shown at the leading lamella (arrowheads) as the cell moves gradually to the lower left, as oriented in this figure. The second dark ring in these images shows an abrupt change in contrast. Near the trailing cell processes it is quite dark (solid arrows), while in the leading lamella it is much less distinct (open arrows). The difference in ring contrast between the two regions may be caused by a difference in cellular impedance (stiffness-density product). The motile behavior of this cell may have resulted in increased stiffness or density, or both, in the trailing processes relative to the leading lamella. The images are taken at focus $Z = 0$ on a quarterwave glass-on-sapphire substratum. Bar = 20 μm.

this interpretation (unpublished data).

Fig. 9 shows a cell spreading toward the lower left as oriented in the figure. The spreading region (leading lamella) appears as a characteristic broad sheet of cytoplasm (13). The trailing portions of the cell are toward the top and right. The images were taken at the $Z = 0$ position on a glass-on-sapphire substratum (see Fig. 6). A pattern of rings is observed which may be correlated with cell topography, as described earlier. An abrupt change in intensity occurs along the second dark ring. In regions of the cell near the extended trailing processes, the ring is quite dark (Fig. 9, solid arrows), while in the leading lamella the ring is much less distinct (Fig. 9, open arrows). If the intensity ratio of this dark ring and the next enclosed bright ring is compared across the cell, the trailing regions have enhanced ring contrast relative to the leading lamella. Our interpretation is that the difference in ring contrast results from a difference in cellular impedance (stiffness-density product). A region of greater cellular impedance gives a larger acoustic reflection from the top of the cell and, hence, more ring contrast.

We suggest that the motile behavior of this cell has resulted in greater impedance in the trailing portion of the cell relative to the leading lamella. Although an impedance change may result from changes of either stiffness or density, or both, the morphology of motile cells suggests a stiffening of the trailing processes. It has been pointed out that trailing cell processes may be under tension (14), corresponding to stretching as the rest of the cell moves away.

CONCLUSION

We have shown that the reflection acoustic microscope can image living cells at submicrometer resolution. Some of the features observed such as nucleoli, ruffles, and intracellular particles are familiar to phase-contrast microscopy. Dark streaks are seen that appear to correspond to the reduced cell-substratum separation observed in interference-reflection microscopy. Other observations, such as the proposed variation of impedance in the actively motile cell of Fig. 9, may give new information on cellular elastic properties. A variety of different techniques have been used in attempts to measure mechanical properties associated with cell motility. For example, birefringence induced in streaming endoplasm was used as an indicator of viscoelasticity (15). Likewise, traction forces exerted by cells were studied by examining the folding of a thin silicon rubber substratum (16). However, the acoustic microscope appears to provide a relatively direct means of studying the elastic state in localized regions within living cells.

We thank Abdullah Atalar for valuable help in the early stages of this project. In particular, he produced the images that appear in Fig. 5. We are grateful to Norman Wessells for allowing us to use his laboratory for the culturing of cells. This work was supported by Research Grant 1 R01 GM-25826-02 from the National Institutes of Health.

1. Johnston, R. N., Atalar, A., Heiserman, J., Jipson, V. & Quate, C. F. (1979) *Proc. Natl. Acad. Sci. USA* **76,** 3325–3329.
2. Rugar, D., Heiserman, J., Minden, S. & Quate, C. F. (1980) *J. Microsc.* **120,** 193–199.
3. Lemons, R. A. & Quate, C. F. (1974) *Appl. Phys. Lett.* **24,** 163–165.
4. Jipson, V. & Quate, C. F. (1978) *Appl. Phys. Lett.* **32,** 789–791.
5. Lemons, R. A. & Quate, C. F. (1979) in *Physical Acoustics*, ed. Thurston, R. N. (Academic, New York), Vol. 14, pp. 1–92.
6. Atalar, A. (1978) *J. Appl. Phys.* **49,** 5130–5139.
7. Weglein, R. D. (1979) *Appl. Phys. Lett.* **34,** 179–181.
8. Haemmerli, G., Strauli, P. & Ploem, J. S. (1980) *Exp. Cell Res.* **128,** 249–256.
9. Trinkaus, J. P. (1976) in *The Cell Surface in Animal Embryogenesis and Development*, eds. Poste, G. & Nicolson, G. L. (North-Holland, New York), pp. 225–311.
10. Harris, A. (1969) *J. Cell Biol.* **43,** 165a.
11. Buckley, I. K. (1973) *Lab. Invest.* **29,** 411–421.
12. Izzard, C. S. & Lochner, L. R. (1976) *J. Cell Sci.* **21,** 129–159.
13. Abercrombie, M., Heaysman, J. E. & Pegrum, S. M. (1971) *Exp. Cell Res.* **67,** 359–367.
14. Trinkaus, J. P., Betchaku, T. & Krukilowski, L. S. (1971) *Exp. Cell. Res.* **64,** 291–300.
15. Francis, D. W. & Allen, R. D. (1971) *J. Mechanochem. Cell Motil.* **1,** 1–6.
16. Harris, A. K., Wild, P. & Stopak, D. (1980) *Science* **208,** 177–179.